Carbohydrates

How to cite:
International Edition: doi.org/10.1002/anie.202105729
German Edition: doi.org/10.1002/ange.202105729

Glycopolymer Microarrays with Sub-Femtomolar Avidity for Glycan Binding Proteins Prepared by Grafted-To/Grafted-From Photopolymerizations

*Daniel J. Valles, Yerzhan S. Zholdassov, Joanna Korpanty, Samiha Uddin, Yasir Naeem, David R. Mootoo, Nathan C. Gianneschi, and Adam B. Braunschweig**

Abstract: *We report a novel glycan array architecture that binds the mannose-specific glycan binding protein, concanavalin A (ConA), with sub-femtomolar avidity. A new radical photopolymerization developed specifically for this application combines the grafted-from thiol–(meth)acrylate polymerization with thiol–ene chemistry to graft glycans to the growing polymer brushes. The propagation of the brushes was studied by carrying out this grafted-to/grafted-from radical photopolymerization (GTGFRP) at > 400 different conditions using hypersurface photolithography, a printing strategy that substantially accelerates reaction discovery and optimization on surfaces. The effect of brush height and the grafting density of mannosides on the binding of ConA to the brushes was studied systematically, and we found that multivalent and cooperative binding account for the unprecedented sensitivity of the GTGFRP brushes. This study further demonstrates the ease with which new chemistry can be tailored for an application as a result of the advantages of hypersurface photolithography.*

Introduction

Glycan microarrays[1] are composed of substrates patterned with monosaccharides or polysaccharides and are used to study the carbohydrate binding specificity of proteins[2] and antibodies,[3] or to identify potential drug targets.[4] Alternatively, glycan microarrays are used as sensors to detect the presence of carbohydrate-binding biomarkers that may indicate disease states.[5] As such, glycan microarrays are becoming one of the most promising tools in the rapidly growing field of chemical glycobiology that seeks to interrogate the role of carbohydrates in biology.[6] Despite their promise, glycan microarrays are not nearly as widely used as DNA microarrays or antibody microarrays in the context of sensors or fundamental science because of several persistent and unresolved challenges. The first is the relatively weak binding affinity between glycans and glycan binding proteins (GBPs) that limits sensitivity and precludes binding of GBPs to the microarrays at biologically relevant concentrations. In solution, the 1:1 binding affinity between glycans and GBPs is typically on the order of 10^{-3}–10^{-5} M, which is substantially weaker than the typical binding between complementary DNA strands, enzymes and their substrates, or antibodies and their targets (frequently $< 10^{-9}$ M). Because of the sensitive dependence of GBP binding in microarrays to glycan density and linker composition, the binding may be even weaker than in solution.[7] In the glycocalyx, the 100 nm–1 μm layer of glycans on the surface of cells and many viruses, this weak binding is overcome by the dense, multivalent presentation of oligoglycans and glycopolymers, and, as a result of the cluster-glycoside effect,[8] can decrease the apparent dissociation constant (K_d) by up to six orders of magnitude.[9] Thus, to reproduce the binding modes that occur in biology and to detect GBPs at biologically relevant concentrations, glycan microarrays should reflect more accurately the multivalent presentation of glycans in the glycocalyx. The other major limitation to the widespread adoption of glycan microarrays is the difficulty associated with immobilizing carbohydrates onto surfaces, as doing so often requires difficult and multi-

[*] D. J. Valles, Y. S. Zholdassov, Prof. D. R. Mootoo, Prof. A. B. Braunschweig
The PhD program in Chemistry
Graduate Center of the City University of New York
365 5th Ave, New York, NY 10016 (USA)
E-mail: ABraunschweig@gc.cuny.edu
D. J. Valles, Y. S. Zholdassov, S. Uddin, Y. Naeem, Prof. A. B. Braunschweig
Advanced Science Research Center at the Graduate Center
The City University of New York
85 St. Nicholas Terrace, New York, NY 10031 (USA)
D. J. Valles, Y. S. Zholdassov, S. Uddin, Y. Naeem, Prof. D. R. Mootoo, Prof. A. B. Braunschweig
Department of Chemistry, Hunter College
695 Park Ave, New York, NY 10065 (USA)
J. Korpanty, Prof. N. C. Gianneschi
Department of Chemistry, Northwestern University
Evanston, IL 60208 (USA)
Prof. N. C. Gianneschi
Department of Materials Science and Engineering
Northwestern University
Evanston, IL 60208 (USA)
and
Department of Biomedical Engineering
Northwestern University
Evanston, IL 60208 (USA)
Prof. A. B. Braunschweig
The PhD program in Biochemistry
Graduate Center of the City University of New York
365 5th Ave, New York, NY 10016 (USA)

Supporting information (detailed description of organic synthesis and characterization, thiol-terminated substrate preparation, AFM analysis, XPS analysis, micro-FTIR analysis, fluorescence analysis, K_d analysis, scanning electron microscope (SEM), references) and the ORCID identification number(s) for the author(s) of this article can be found under: https://doi.org/10.1002/anie.202105729.

step synthetic modification of the carbohydrates. Ideally, the approaches to create the glycan arrays should address both major challenges by enabling the facile integration of widely available glycans onto multivalent scaffolds.

Inspired by the polymeric backbone, high glycan density, and rigid extended structures of cell-surface mucins—the heavily glycosylated lipoproteins that coat cell surfaces[10]—researchers have recently leveraged cutting-edge polymer chemistries to create microarrays containing multivalent glycopolymer brushes. In an initial demonstration of the effectiveness of this approach, the Gildersleeve group conjugated bovine serum albumin (BSA) modified with carbohydrates onto epoxide-modified glass slides.[11] In doing so, they found that neoglycoproteins with larger glycan density displayed smaller K_d values. To test how multivalency affects binding between mannose and the mannose-binding GBP, concanavalin A (ConA), they also altered the density of mannose-modified BSA on the surface.[12] They found that without spacing, K_d was 69 nM, but upon spacing them sufficiently with inert BSA, ConA does not bind to the microarray. These data suggest that at least two of the four ConA binding sites must be occupied for the protein to adhere to the microarray. Bertozzi and Godula[13] prepared glycopolymers using reversible addition–fragmentation chain-transfer (RAFT) polymerization to mimic the natural glycan presentation of cell-surface mucins in synthetic polymers. Aminooxy-labelled α-*N*-acetylgalactosamine was grafted at different densities and onto polymer chains of different lengths, which were then immobilized into microarrays to examine how density affected association, resulting in K_ds from 1 to 500 nM. Godula also polymerized Boc-protected *N*-methylaminooxypropylacrylamide. Removal of the Boc-groups reveals amine conjugation sites for aminooxy-containing glycans.[14] With these polymers they detected influenza A virus hemagglutinin (HA) at 5 HAU mL^{-1}, which was substantially more sensitive than arrays prepared with monolayers of glycans. In another example of post-polymerization glycosylation, Neumann et al. capitalized on thiol–ene click chemistry to conjugate thiol-functionalized glycans at different densities to alkene side-groups in poly(allyl glycidyl ether), and then grafted the terminal hydroxy group of the glycopolymer to isocyanate-functionalized glass substrates. The glycopolymer arrays were assayed against the ConA to determine K_d.[15] They found that as the density of glycans on the polymers increased, K_d of the GBP decreased accordingly, with K_d values as low as 27 nM for the binding between galactose-modified glycopolymers and the galactose-specific GBP, *Ricinus communis agglutin I*. All of these assays demonstrate the increase in binding strength with increasing valency, but by grafting the polymers to the microarray substrates, these approaches required complex syntheses and architectures that are limited to relatively flexible, linear chains.[16]

An alternate approach to creating glycopolymer microarrays involves grafting-from reactions to grow glycopolymers directly from the substrate, an approach whose advantages include greater control over surface density, simpler syntheses, and a greater ability to manipulate glycan presentation. Our group has explored a variety of surface chemistries[17] including, but not limited to, grafted-from thiol–ene[18] and thiol–(meth)acrylate[19] photoreactions for preparing multiplexed monolayer glycan microarrays[18] and grafted-from glycopolymer arrays[20] to investigate how valency, brush height, and spacing affect GBP binding. We found that binding to ConA was substantially greater for glycan-modified polymers than that for monolayers, but the printing approach we employed was not able to control feature height, architecture, and density simultaneously. Despite the promise of grafted-from chemistry on glycan microarrays, new tools and chemistries for creating glycan microarrays are needed where multivalency and polymer height can each be independently controlled. With such tools, researchers can reproduce the architecture of the glycocalyx, and thereby interrogate biological recognition and increase sensitivity. Here we combine advanced photolithography with new polymer chemistry to create multiplexed glycan microarrays that reproduce the dense glycan presentation found in the glycocalyx. To accomplish this, we combine a recently reported photochemical printing method, "Hypersurface Photolithography" (HP),[21] with a reaction that we term "grafted-to/grafted-from radical photopolymerization" (GTGFRP, Scheme 1), in which the glycans are grafted to

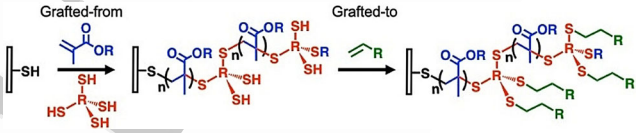

Scheme 1. Grafted-to/grafted-from radical photopolymerization initiated from a thiol-functionalized surface. The EGDMA and PETT copolymer is grafted from the surface, while alkene-labelled Man-5 are grafted to the free thiols from PETT.

a polymer chain as it grows grafted from a surface (Figure 1), and use the resulting glycan microarrays to explore systematically the role of grafting density and polymer height on K_d. The result of these efforts is a powerful new approach for creating glycan microarrays, a fuller understanding of how glycopolymer architecture can be modulated to control K_d, and multiplexed glycopolymer microarrays with sub-1 fM K_ds to ConA—the strongest binding between GBPs and glycan arrays yet reported.

Results and Discussion

This study is enabled by the HP[21a,c] printing platform (Figure 1a) that is used to rapidly assess how reaction conditions affect the growth rates of grafted-from polymer brushes. HP combines microfluidics, a 405 nm LED, and a digital micromirror device (DMD) with ≈700000 individually addressable mirrors[22] to create multiplexed polymer arrays. Microfluidics coordinate delivery of reagents to a fluid cell, where photochemical reactions occur between reagents in solution and an appropriately functionalized surface. Previously, we have used this printer to study the kinetics of surface-initiated atom transfer radical photopolymerization (SI-ATRP)[21c] and the thiol–(meth)acrylate photopolymer-

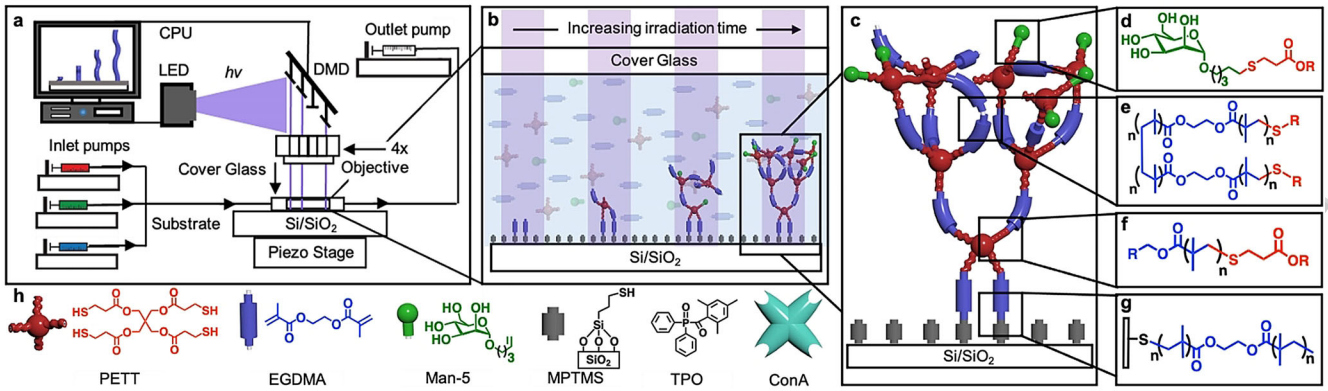

Figure 1. a) Hypersurface photolithography printer equipped with a CPU-controlled digital micromirror device (DMD) and a 405 nm LED. Microfluidic pumps deliver and remove the printing solution from the reaction chamber. b) Polymer brushes grow from the surface by consuming monomers in solution upon exposure to light (purple lines). Increasing irradiation times result in polymer brushes with increasing heights. c) The grafted-to/grafted-from radical polymerization produces microscopically heterogeneous cross-linked polymer brushes with different chemical bonds (d–g). h) The chemical structures of reagents used in the polymerizations.

ization[21b] and to make stimuli-responsive surfaces that reveal hidden messages.[21a] Each of these examples illustrates the major advantages of this printer—the acceleration of reaction discovery and optimization of grafted-from kinetics—because each of the pixels in a pattern can be composed of a polymer that is printed under a different condition, where factors that affect growth, such as irradiation time, reagents, or light intensity, can be varied systematically. In addition, each pattern can be repeated hundreds of times across the surface leading to statistically significant data and minimized batch-to-batch variability. As a consequence, a kinetic model of grafted-from polymerizations can be derived so the architectures of the features in a pattern can be precisely controlled. This reaction discovery and printing approach is a major shift in how polymer brush chemistry is performed in that grafted-from chemistries that are tailored to a specific application can be rapidly developed and complex multiplexed patterns can be printed, such that each pixel has a unique chemical composition and height.

Here we apply HP to develop an entirely new polymerization, the GTGFRP, that has been specifically designed for making ultrasensitive glycopolymer microarrays. We had shown previously[19b,23] that methacrylate polymer brushes could be photochemically grafted from surface-bound thiols in an inert atmosphere in the presence of diphenyl(2,4,6-trimethylbenzoyl)phosphine oxide (TPO) and $Ir(ppy)_3$ via a radical propagation mechanism.[21b] Heights of the resulting polymers, however, did not exceed 30 nm, there was no straightforward approach to incorporate glycans, and the necessity for an inert atmosphere complicated printing. Multiple groups[24] have popularized a variant of the photochemical thiol–(meth)acrylate polymerization in which pentaerythritol tetrakis(3-mercaptopropionate) (PETT) is combined with a monomer containing multiple methacrylate groups, which leads to a highly cross-linked polymer. In parallel, we and others have immobilized glycans into microarrays using the photoreaction between surface-bound thiols and alkene-modified glycans.[18a,b] This latter reaction is particularly well suited for glycan microarrays because alkenes are common glycan protecting groups, and, as a consequence, are easy to prepare and are widely available.[25] Further, the thiol–ene reaction is bioorthogonal,[23] not requiring that the hydroxy groups are protected. Thus, our new polymerization design is a combination of these three photoreactions—the grafted-from polymerization from a thiol-terminated surface, the thiol–acrylate polymerization, and the thiol–alkene reaction—all occurring simultaneously to create polymer brush scaffolds with projecting glycans, where the heights and glycan densities can be controlled independently.

Before we created the glycan-containing polymer brushes, we set out to demonstrate that this photoreaction could be used to create polymer brushes with controlled heights and to determine how the concentration of each of the different reagents—[PETT], [ethylene glycol dimethacrylate] ([EGDMA]), and [TPO]—and light intensity (hv) affect growth rate. To carry out each print, thiol-terminated Si < 100 > wafers[21b] were placed into the fluid cell. Using microfluidics, the printing solutions containing the three reactive components, dissolved into DMSO, were introduced into the fluid cell so they were in direct contact with the thiol-functionalized Si-substrate. It should also be noted that all solutions were prepared under ambient conditions, without making efforts to degas or rigorously exclude water. Patterns containing 16 features with dimensions of $10 \times 10\ \mu m^2$ were projected onto the surface by the DMD, where each feature in each of the 250 identical patterns was illuminated for a different time, t (1–16 min). Following printing, the substrates were washed with DMSO, EtOH, and sonicated in DMSO for 5 min to remove any physisorbed polymer. The presence of patterns was confirmed by optical microscopy (Figure 2b,c), and the heights, h, of the features were measured by atomic force microscopy (AFM, Figure 2d).

To explore the brush growth rates, a set of surfaces were patterned, where, in each surface, a single parameter is varied and all others are held constant. First, the [EGDMA] was varied from 520 to 1560 mM, while [TPO], hv, and [PETT] were held constant (Figure 2e). We observed that the

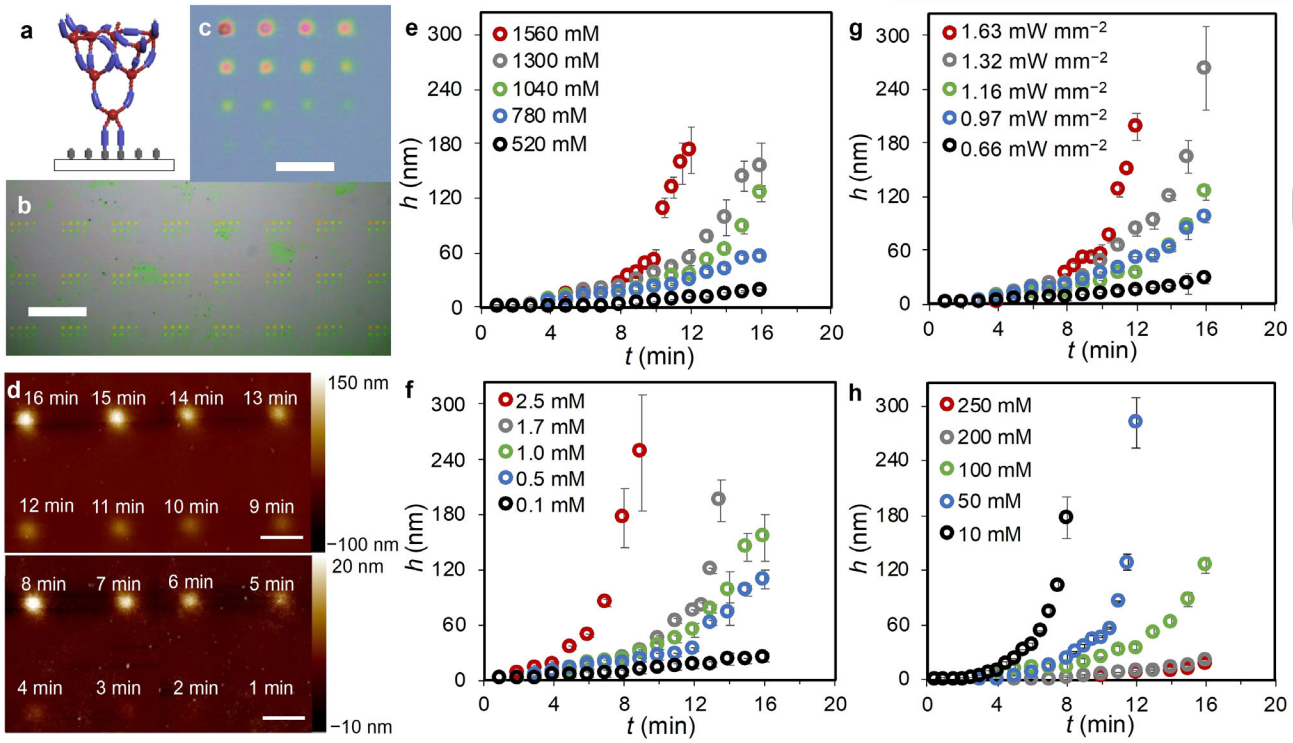

Figure 2. a) Representation of brush grown with EGDMA and PETT monomers. b) Optical microscopy image (10×) of a polymer brush pattern ([EGDMA] = 1300 mM, [TPO] = 1 mM; light intensity = 1.16 mW mm^{-2}; [PETT] = 100 mM). Scale bar is 250 μm. c) Optical image (40×) of a single polymer brush pattern, where *t* varies from 1 to 16 min. Scale bar is 50 μm. d) AFM analysis of polymer brush height. The scale bar is 20 μm. Heights are reported as the average of 3 features of the same exposure time, and all error bars are reported as one standard deviation from the mean. e) Effect of varying [EGDMA] on brush growth ([TPO] = 1 mM; light intensity = 1.16 mW mm^{-2}; [PETT] = 100 mM). f) Effect of varying [TPO] on brush growth ([EGDMA] = 1300 mM; light intensity = 1.16 mW mm^{-2}; [PETT] = 100 mM). g) Effect of varying light intensity on brush growth ([EGDMA] = 1300 mM; [TPO] = 1 mM; [PETT] = 100 mM). h) Effect of varying [PETT] on brush growth ([EGDMA] = 1300 mM; [TPO] = 1 mM; light intensity = 1.16 mW mm^{-2}).

polymer brush *h* increased with increasing [EGDMA] and also that the *h* grew exponentially with *t*. Similar trends were observed when we examined [TPO] (Figure 2f) and *hν* (Figure 2g). Brush *h* that exceeded the *z*-resolution of the AFM (1 μm) were frequently observed and were not included in the plots. These observations differ substantially from the trends we observed in studying polymer grown by SI-ATRP[21c] or the propagation of methacrylates from thiol surfaces.[21b] In the previous cases, *h* increased linearly with *t* until stopping abruptly, which is commonly observed in brush polymerizations.[21b,c] Furthermore, $h > 30$ nm were never observed for the thiol–methacrylate polymerization,[21b] whereas here features $\gg 1$ μm tall are regularly produced by the GTGFRP. We had observed previously that there were thresholds for [TPO] or *hν*, above which growth slowed or stopped altogether. There were no such limits observed here within the concentration ranges examined. In contrast to the other components, we found that increasing [PETT] decreases growth rate (Figure 2h). To explain these data, we attribute the exponential growth rate to the continuous initiation from new sites as PETT is incorporated into the growing chain, which both precludes chain-termination and increases growth rates as the number of living ends multiplies over time in a pseudo-dendritic fashion. The decrease in growth rate with increasing [PETT] could be explained by any of the following reasons: (1) Increasing rate of termination as a result of disulfide formation or other chain–chain reactions, (2) as more PETT is incorporated into the chain, the reactive radical sites are thiol radicals rather than propagating methacrylates, and initiation of a new chain is much slower than methacrylate propagation, or (3) polymers growing in solution are outcompeting the surface-bound brushes for limited monomer in solution, although this seems least likely as the monomer is present in solution in large excess. Further investigation is needed to understand fully the kinetics of this reaction, but the studies presented here reveal interesting subtleties that govern the kinetics of this complex GTGFRP.

We next investigated how the introduction of the alkene-functionalized glycan, pent-4-enyl-α-D-mannopyranoside (Man-5) into the reactive solution affected polymer growth rate and confirmed that the glycan is incorporated into the growing brushes. To do so, we printed the same 16-feature patterns onto the thiol-terminated substrates (Figure 3b), and [Man-5] was varied from 0–500 μM (Figure 3c). Glycan incorporation into these polymer brushes was confirmed by XPS and micro-FTIR analysis. XPS analysis of the C1s spectra of four different surfaces were compared. Surface polymers composed of EGDMA and EGMDA with PETT displayed similar peaks, but after incorporating Man-5, a new peak emerged at 287.4 eV indicating C–OH bonding (Fig-

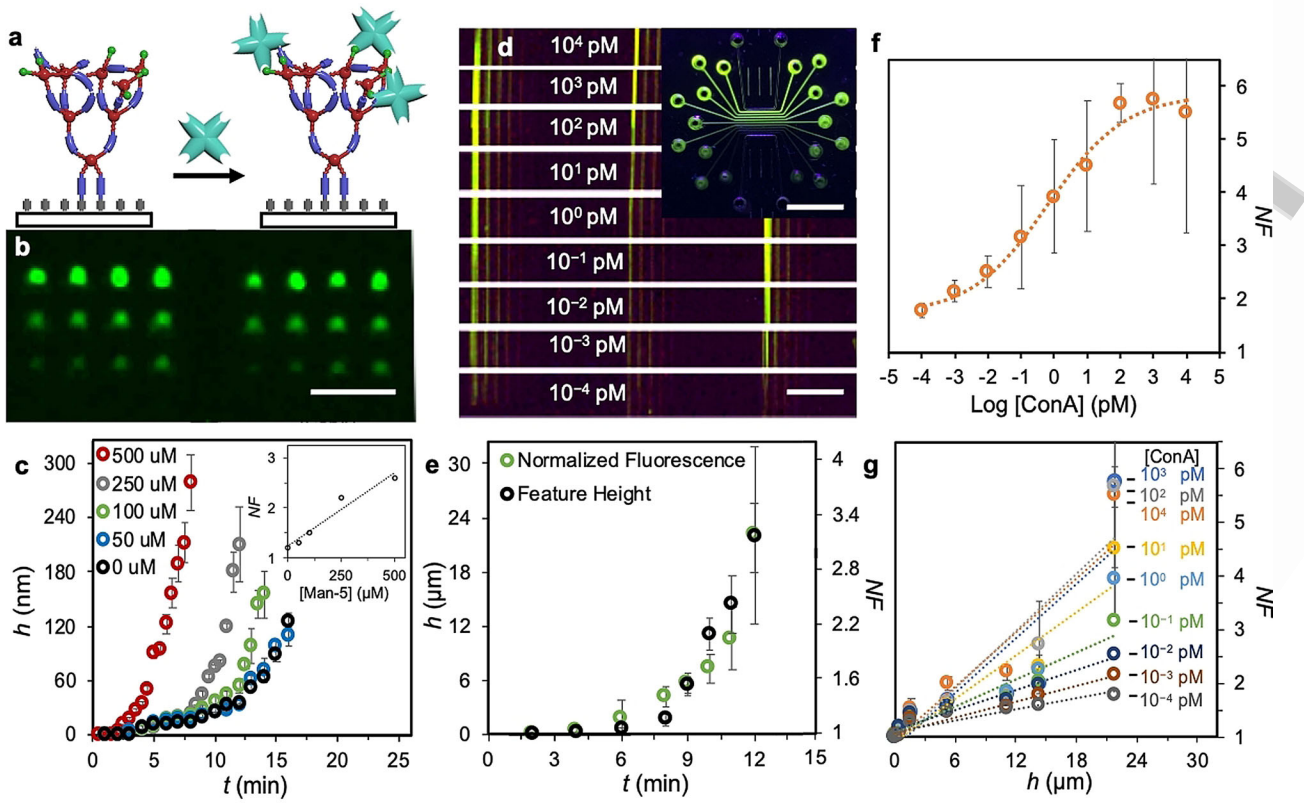

Figure 3. a) ConA binding to the Man-5-containing GTGFRP brushes. b) Fluorescence microscopy of FITC-ConA bound to Man-5-containing GTGFRP brushes. Scale bar is 100 μm. c) Effect of varying [Man-5] on GTGFRP polymer growth rate ([EGDMA] = 1300 mM; [TPO] = 1 mM; light intensity = 1.16 mW mm^{-2}; [PETT] = 100 mM). The inset shows the effect of varying [Man-5] on fluorescence with polymer brushes with heights of 110 ± 10 nm. d) Fluorescence image of Man-5-containing GTGFRP brushes of varying heights patterned into vertical lines after exposure to FITC-ConA. Scale bar is 300 μm. Inset is a fluorescence image of the incubation chip contained ■containing■ FITC-ConA solutions at 9 different concentrations. Scale bar is 5 mm. e) The height and *NF* of the vertical line pattern of Man-5-containing GTGFRP glycopolymers from the channel with 0.1 pM FITC-ConA. f) Relationship between [ConA] and *NF* for feature heights of 22 ± 3.8 μm. g) Relationship between height Man-5 and *NF* of Man-5-containing GTGFRP polymers upon exposure to solutions with different [FITC-ConA]. Heights are reported as the average of 3 features of the same exposure time, and all error bars are reported as one standard deviation from the mean.

ure S43). Micro-FTIR revealed that spectra of the features in surfaces printed in the presence and absence of Man-5 displayed sharp/strong bands at 2947 and 1720 cm^{-1}, likely arising from C−H and C=O stretching, respectively. Surfaces printed in the presence of Man-5 possessed an additional broad band at 3430–3630 cm^{-1} that can be attributed to O−H groups in the glycan (Figure S47). In assessing how reaction conditions affected growth-rate, we observed the same exponential growth with increasing time, and, interestingly, we found that the presence of [Man-5] increased growth rate substantially when compared to polymerizations carried out in its absence (Figure 3c). It is unclear why increasing [Man-5] accelerates growth and is another curious aspect of this polymerization that should be explored further. The surfaces were then exposed to fluorescein isothiocyanate (FITC)-labelled ConA to examine how the change in glycan density on the polymer brushes affect binding. To do so, the surfaces were passivated in a 1% (w/v) solution of BSA for 30 min, then they were washed with MilliQ water and dried under a stream of air before being incubated in a solution of FITC-ConA for 12 hours. The surfaces were washed three times for 10 min each in fresh solutions of MilliQ water with 0.01% Tween20 and dried under a stream of air. The results (Figure S42) show that when no glycan is present on the polymer there is no visible fluorescence pattern. Fluorescence increases linearly with increasing [Man-5] in the reactive solution, even while the *h* of the brushes is held constant (Figure 3c, inset), demonstrating that the grafting density of [Man-5] is clearly increasing in the polymer brushes. Finally, surfaces patterned at [Man-5] = 500 μM and controls that were printed without Man-5, were incubated in solutions containing FITC-labelled ConA, or DyLight 594-labeled *griffonia simplicifolia I* (GSL), a galactose-specific GBP that does not bind mannosides. Strong fluorescence with low background was observed only on the surface patterned with Man-5 that was incubated with FITC-ConA, whereas no significant fluorescence was observed in any other experiment (Figure S34). Fluorescence values of the GSL binding experiment at high protein concentration were small ($NF < 1.2$) and near the background threshold. Taken together, these data confirm the successful grafting-to of Man-5 onto the growing polymer brushes, that *h* can be controlled even in the presence of the glycan, and that native binding specificity is maintained.

A series of assays were carried out to examine the relationships between polymer architecture and their binding to FITC-ConA. Patterns of 8 vertical lines (Figure S48a) of [Man-5]-containing brushes were prepared, with each line printed at a different t (2–12 min). The h of the polymer brushes were analyzed by profilometry (Figure S48b,c), and range in h from 22 to 0.01 μm. Previously,[18a,b] our group reported a microfluidic chip that contains 11 channels, each 250 μm wide, for the purpose of testing simultaneously the binding of the microarray to various GBP solutions (Figure 3d, inset). This chip was placed onto the pattern, orienting the channels of the chip perpendicular to the patterned polymer brush lines. Then, 9 solutions of FITC-ConA, at concentrations ranging from 10^4 to 10^{-4} pM, were injected into the different channels and incubated for 12 hours. Binding was assessed by fluorescence microscopy (Figure 3d), and the post-incubation h were measured by profilometry (Figure 3e). There was no significant change in line h after binding (Figure S47), suggesting that the highly cross-linked polymers are relatively stiff and do not change after binding, which is different to what we have observed with linear polymers.[20] We also found that fluorescence increases as [ConA] increases (Figure 3e,f), and that fluorescence also increases with increasing h (Figure 3g). Using the fluorescence data, we applied the Langmuir isotherm approach[11–13,15,26] to determine the K_ds between ConA and the glycopolymer brushes (Table S29) for all 72 combinations of brushes and ConA solutions. We observed decreasing K_d with increasing glycan density and increasing h. In our previous report,[18a] the lowest [ConA] observed to bind to Man-5 monolayers was at a [ConA] of 48 nM with a K_d of 28 nM, while here, the lowest [ConA] observed to bind to Man-5 glycopolymers was at a solution concentration of 10^{-4} pM with a K_d of 0.3 fM, resulting in binding that is 10^{-7} M stronger than the monolayers of Man-5.[18a,b] These K_ds are $\approx 10^{-7}$ M lower than galactosides grafted to linear polymers by aminooxy conjugation,[13a] and 10^{-8} M lower than the binding of *ricinus communis agglutinin I* to galactosides bound to linear polymers via thiol–ene photochemistry.[27] The fluorescence values were also used quantitatively to analyze the binding cooperativity of ConA with the surface glycopolymer. The isotherm was fit to a 4-parameter logistic model[28] [Eq. (S3)], which has been widely applied to analyze surface binding.[29] The Hill coefficient was determined to be −0.37 (Table S30), whose value of <1 indicates negative cooperativity in binding that is in good agreement with prior reports that ConA binds with negative cooperativity to polyvalent ligands.[13a,30]

We attribute the ultrasensitive detection of FITC-ConA to two factors unique to the cross-linked GTGFRP brush architectures. The first is that fluorescence increases in taller polymers as there are simply more proteins bound into the taller stacks, so signal increases with increasing polymer brush h as a result of multivalency. The exponential growth kinetics result in polymer brushes that are far taller than typical linear glycopolymer brushes, so the increase in signal as a result of increased h is substantial (Figure 4a). The second is that binding itself is stronger, which arises for two reasons. ConA has four identical binding sites and it is well-known that

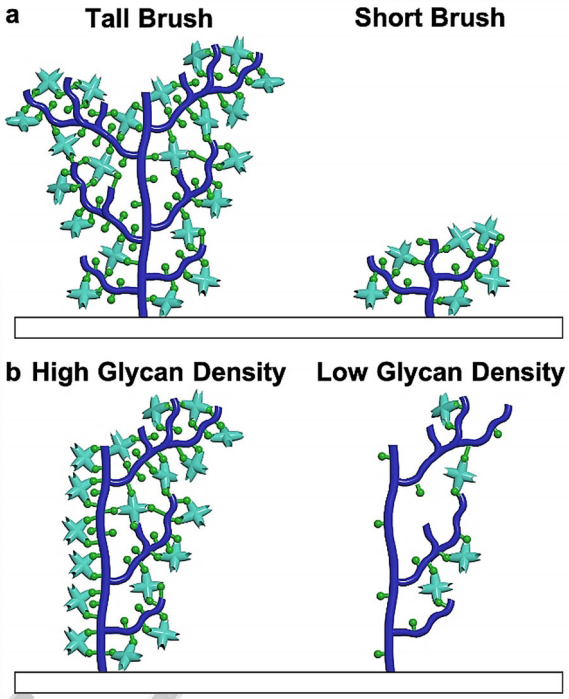

Figure 4. Avidity depends upon a) multivalency, where taller polymers provide more Man-5 binding sites for ConA, and b) cooperativity, where lower [Man-5] in the printing solution leads to lower density of glycan on the polymer. The decrease in mannose presented on the polymer, along with the increased spacing between them, leads to a significant decrease in ConA binding because fewer binding sites in the GBP are occupied.

binding strength increases when this GBP can bind multivalently.[31] As grafting density and branching increases in these dense and cross-linked pillars, it is likely that all four sites can become occupied with mannosides, which would strongly anchor the GBPs to the polymer brushes as a result of cooperativity between the binding sites (Figure 4b). This is consistent with the work of Gildersleeve[12] and our own[18a] that shows that at least two sites on the ConA should be occupied by mannose to achieve binding to the microarray. The other reason why binding strength may increase compared to other glycopolymer systems is that the dense, crosslinked brushes are highly preorganized, as evidenced by the consistent h before and after binding, which likely decreases the entropic penalty of association, which has been shown to play an important role in GBP-glycan recognition.[32]

Conclusion

We report a new microarray architecture for detecting GBP binding with sub-fM avidity, the strongest binding between GBPs and microarrays yet reported. This performance is the direct result of new chemistry, that combines free-radical polymerizations with thiol–ene click reactions, whose advantages are controllable feature heights over a range of <10 nm–>20 μm, the easy incorporation of glycans, and tailorable glycan grafting density. The rapid

Dateiname: F105729e
Pfad: l:/daten/verlage/vch/ach/hefte/pool/
Status Neusatz
Datum: 32 KW., 3. August 2021 (Dienstag)
Pagina: 7
Seite: 6 te von 10
Umfang (Seiten): 10
Zeit: 7:10:24 Uhr

development of this new chemistry and the systematic investigation of brush height and grafting density are all enabled by a new chemical printer that accelerates the discovery and optimization timeline, which is demonstrated herein by the >400 different reaction conditions for growing the polymer brushes whose growth and binding were analyzed. Quantitative binding studies explain the cause of the unprecedented avidity to these polymer brushes. This is a direct result of the brush structures produced by GTGFRP that eschews microscopic homogeneity for architectures that reproduce glycan presentation in the glycocalyx more accurately. The new chemistry and the understanding of the underlying binding process that we report could usher in a new era in glycobiology, where glycan-binding proteins can now be detected at medically and biologically relevant concentrations. In addition, this work is a milestone in a new era of brush polymer chemistry, where, as a result of hypersurface photolithography, new brush polymer chemistries and architectures can be rapidly developed and optimized to meet the needs of emerging applications.

Acknowledgements

This work was supported by funding from the Air Force Office of Scientific Research (FA9550-19-1-0356), the Army Research Office (W911NF-17-1-0326), the National Science Foundation (DBI-2032176, CHE-1905270, CHE-1900509), the Army Research Office (W911NF-15-1-0568), and the Department of Defense (MURI 15RT0675). We would like to acknowledge the Surface Science Facility and the Imaging Facility of CUNY Advanced Science Research Center for instrumentation used to characterize the surfaces. The National Science Foundation (CHE 1828399) for the NEO-500 NMR spectrometer used to obtain data included in this publication; the Keck-II facility of Northwestern University's NUANCE Center, which has received support from the SHyNE Resource (NSF ECCS-2025633), the International Institute for Nanotechnology at Northwestern University, and Northwestern's MRSEC program (NSF DMR-1720139).

Conflict of Interest

The authors declare no conflict of interest.

Keywords: glycopolymers · lectins · lithography · microarrays · thiol–ene

[1] a) O. Oyelaran, J. C. Gildersleeve, *Curr. Opin. Chem. Biol.* **2009**, *13*, 406 – 413; b) J. Stevens, O. Blixt, J. C. Paulson, I. A. Wilson, *Nat. Rev. Microbiol.* **2006**, *4*, 857 – 864.

[2] a) C. Gao, M. Wei, T. R. McKitrick, A. M. McQuillan, J. Heimburg-Molinaro, R. D. Cummings, *Front. Chem.* **2019**, *7*, 0 ■■article number?■■; b) C. D. Rillahan, J. C. Paulson, *Annu. Rev. Biochem.* **2011**, *80*, 797 – 823.

[3] Y. Zhang, C. Campbell, Q. Li, J. C. Gildersleeve, *Mol. Biosyst.* **2010**, *6*, 1583 – 1591.

[4] B. Ernst, J. L. Magnani, *Nat. Rev. Drug Discovery* **2009**, *8*, 661 – 677.

[5] a) M. L. Huang, M. Cohen, C. J. Fisher, R. T. Schooley, P. Gagneux, K. Godula, *Chem. Commun.* **2015**, *51*, 5326 – 5329; b) R. A. Childs, A. S. Palma, S. Wharton, T. Matrosovich, Y. Liu, W. Chai, M. A. Campanero-Rhodes, Y. Zhang, M. Eickmann, M. Kiso, A. Hay, M. Matrosovich, T. Feizi, *Nat. Biotechnol.* **2009**, *27*, 797 – 799.

[6] A. Varki, *Essentials of glycobiology*, 2nd ed., Cold Spring Harbor Laboratory Press, Cold Spring Harbor, **2009**.

[7] J. S. Temme, C. T. Campbell, J. C. Gildersleeve, *Faraday Discuss.* **2019**, *219*, 90 – 111.

[8] a) J. J. Lundquist, E. J. Toone, *Chem. Rev.* **2002**, *102*, 555 – 578; b) Y. C. Lee, R. T. Lee, *Acc. Chem. Res.* **1995**, *28*, 321 – 327.

[9] a) G. B. Sigal, M. Mammen, G. Dahmann, G. M. Whitesides, *J. Am. Chem. Soc.* **1996**, *118*, 3789 – 3800; b) S.-K. Choi, M. Mammen, G. M. Whitesides, *J. Am. Chem. Soc.* **1997**, *119*, 4103 – 4111.

[10] A. R. Cerullo, T. Y. Lai, B. Allam, A. Baer, W. J. P. Barnes, Z. Barrientos, D. D. Deheyn, D. S. Fudge, J. Gould, M. J. Harrington, M. Holford, C.-S. Hung, G. Jain, G. Mayer, M. Medina, J. Monge-Nájera, T. Napolitano, E. P. Espinosa, S. Schmidt, E. M. Thompson, A. B. Braunschweig, *ACS Biomater. Sci. Eng.* **2020**, *6*, 5377 – 5398.

[11] O. Oyelaran, Q. Li, D. Farnsworth, J. C. Gildersleeve, *J. Proteome Res.* **2009**, *8*, 3529 – 3538.

[12] Y. Zhang, Q. Li, L. G. Rodriguez, J. C. Gildersleeve, *J. Am. Chem. Soc.* **2010**, *132*, 9653 – 9662.

[13] a) K. Godula, C. R. Bertozzi, *J. Am. Chem. Soc.* **2012**, *134*, 15732 – 15742; b) K. Godula, D. Rabuka, K. T. Nam, C. R. Bertozzi, *Angew. Chem. Int. Ed.* **2009**, *48*, 4973 – 4976; *Angew. Chem.* **2009**, *121*, 5073 – 5076; Corrigendum: K. Godula, D. Rabuka, K. T. Nam, C. R. Bertozzi, *Angew. Chem. Int. Ed.* **2012**, *51*, 7881 – 7881; *Angew. Chem.* **2012**, *124*, 8003 – 8003.

[14] M. Cohen, C. J. Fisher, M. L. Huang, L. L. Lindsay, M. Plancarte, W. M. Boyce, K. Godula, P. Gagneux, *Virology* **2016**, *493*, 128 – 135.

[15] A. Gordus, G. MacBeath, *J. Am. Chem. Soc.* **2006**, *128*, 13668 – 13669.

[16] W.-L. Chen, R. Cordero, H. Tran, C. K. Ober, *Macromolecules* **2017**, *50*, 4089 – 4113.

[17] X. M. Liu, C. Carbonell, A. B. Braunschweig, *Chem. Soc. Rev.* **2016**, *45*, 6289 – 6310.

[18] a) D. J. Valles, Y. Naeem, A. Y. Rozenfeld, R. W. Aldasooky, A. M. Wong, C. Carbonell, D. R. Mootoo, A. B. Braunschweig, *Faraday Discuss.* **2019**, *219*, 77 – 89; b) D. J. Valles, Y. Naeem, C. Carbonell, A. M. Wong, D. R. Mootoo, A. B. Braunschweig, *ACS Biomater. Sci. Eng.* **2019**, *5*, 3131 – 3138; c) C. Carbonell, D. J. Valles, A. M. Wong, M. W. Tsui, M. Niang, A. B. Braunschweig, *Chem* **2018**, *4*, 857 – 867.

[19] a) C. E. Hoyle, A. B. Lowe, C. N. Bowman, *Chem. Soc. Rev.* **2010**, *39*, 1355 – 1387; b) A. E. Rydholm, C. N. Bowman, K. S. Anseth, *Biomaterials* **2005**, *26*, 4495 – 4506.

[20] S. Bian, S. B. Zieba, W. Morris, X. Han, D. C. Richter, K. A. Brown, C. A. Mirkin, A. B. Braunschweig, *Chem. Sci.* **2014**, *5*, 2023 – 2030.

[21] a) Y. S. Zholdassov, D. J. Valles, S. Uddin, J. Korpanty, N. C. Gianneschi, A. B. Braunschweig, *Adv. Mater.* **2021**, *33*, 2100803; b) A. M. Wong, D. J. Valles, C. Carbonell, C. L. Chambers, A. Y. Rozenfeld, R. W. Aldasooky, A. B. Braunschweig, *ACS Macro Lett.* **2019**, *8*, 1474 – 1478; c) C. Carbonell, D. J. Valles, A. M. Wong, A. S. Carlini, M. A. Touve, J. Korpanty, N. C. Gianneschi, A. B. Braunschweig, *Nat. Commun.* **2020**, *11*, 1244.

[22] a) B. S. Sumerlin, D. Neugebauer, K. Matyjaszewski, *Macromolecules* **2005**, *38*, 702 – 708; b) J. E. Poelma, B. P. Fors, G. F. Meyers, J. W. Kramer, C. J. Hawker, *Angew. Chem. Int. Ed.* **2013**, *52*, 6844 – 6848; *Angew. Chem.* **2013**, *125*, 6982 – 6986; c) M. Li,

M. Fromel, D. Ranaweera, S. Rocha, C. Boyer, C. W. Pester, *ACS Macro Lett.* **2019**, *8*, 374 – 380.
[23] C. E. Hoyle, C. N. Bowman, *Angew. Chem. Int. Ed.* **2010**, *49*, 1540 – 1573; *Angew. Chem.* **2010**, *122*, 1584 – 1617.
[24] a) J. Tan, C. Li, J. Zhou, C. Yin, B. Zhang, J. Gu, Q. Zhang, *RSC Adv.* **2014**, *4*, 13334 – 13339; b) M.-H. Ryou, Y. M. Lee, K. Y. Cho, G.-B. Han, J.-N. Lee, D. J. Lee, J. W. Choi, J.-K. Park, *Electrochim. Acta* **2012**, *60*, 23 – 30; c) A. K. O'Brien, N. B. Cramer, C. N. Bowman, *J. Polym. Sci. Part A* **2006**, *44*, 2007 – 2014; d) A. Banerji, K. Jin, K. Liu, M. K. Mahanthappa, C. J. Ellison, *Macromolecules* **2019**, *52*, 6662 – 6672.
[25] a) D. R. Mootoo, P. Konradsson, B. Fraserreid, *J. Am. Chem. Soc.* **1989**, *111*, 8540 – 8542; b) D. R. Mootoo, B. Fraser-Reid, *Tetrahedron Lett.* **1989**, *30*, 2363 – 2366.
[26] a) A. J. Haes, R. P. Van Duyne, *J. Am. Chem. Soc.* **2002**, *124*, 10596 – 10604; b) J. C. Riboh, A. J. Haes, A. D. McFarland, C. Ranjit Yonzon, R. P. Van Duyne, *J. Phys. Chem. B* **2003**, *107*, 1772 – 1780; c) H. S. Kojori, Y. W. Ji, Y. Paik, A. B. Braunschweig, S. J. Kim, *Nanoscale* **2016**, *8*, 17357 – 17364.
[27] K. Neumann, A. Conde-González, M. Owens, A. Venturato, Y. Zhang, J. Geng, M. Bradley, *Macromolecules* **2017**, *50*, 6026 – 6031.
[28] Quest Graph™ IC50 Calculator. AAT Bioquest, Inc, 02 Jun. 2021, https://www.aatbio.com/tools/ic50-calculator.
[29] a) C. Klumpp-Thomas, H. Kalish, M. Drew, S. Hunsberger, K. Snead, M. P. Fay, J. Mehalko, A. Shunmugavel, V. Wall, P. Frank, J.-P. Denson, M. Hong, G. Gulten, S. Messing, J. Hicks, S. Michael, W. Gillette, M. D. Hall, M. J. Memoli, D. Esposito, K. Sadtler, *Nat. Commun.* **2021**, *12*, 113; b) E. J. M. Nascimento, J. K. George, M. Velasco, M. I. Bonaparte, L. Zheng, C. A. DiazGranados, E. T. A. Marques, J. W. Huleatt, *J. Virol. Methods* **2018**, *257*, 48 – 57; c) K. Klauenberg, M. Walzel, B. Ebert, C. Elster, *Biostatistics* **2015**, *16*, 454 – 464; d) S. A. Nummer, A. J. Weeden, C. Shaw, B. K. Snyder, T. B. Bridgeman, S. S. Qian, *MethodsX* **2018**, *5*, 304 – 311; e) Y. B. Cheung, Y. Xu, E. J. Remarque, P. Milligan, *J. Immunol. Methods* **2015**, *417*, 115 – 123.
[30] a) T. K. Dam, R. Roy, D. Pagé, C. F. Brewer, *Biochemistry* **2002**, *41*, 1351 – 1358; b) T. K. Dam, R. Roy, D. Pagé, C. F. Brewer, *Biochemistry* **2002**, *41*, 1359 – 1363.
[31] T. K. Dam, R. Roy, S. K. Das, S. Oscarson, C. F. Brewer, *J. Biol. Chem.* **2000**, *275*, 14223 – 14230.
[32] H. Wang, F. Jacobi, J. Waschke, L. Hartmann, H. Löwen, S. Schmidt, *Adv. Funct. Mater.* **2017**, *27*, 1702040.

Manuscript received: April 27, 2021
Revised manuscript received: June 4, 2021
Accepted manuscript online: July 17, 2021
Version of record online: ■■ ■■, ■■■■

Research Articles

Carbohydrates

D. J. Valles, Y. S. Zholdassov, J. Korpanty, S. Uddin, Y. Naeem, D. R. Mootoo, N. C. Gianneschi, A. B. Braunschweig* ——— ■■■■–■■■■

Glycopolymer Microarrays with Sub-Femtomolar Avidity for Glycan Binding Proteins Prepared by Grafted-To/Grafted-From Photopolymerizations

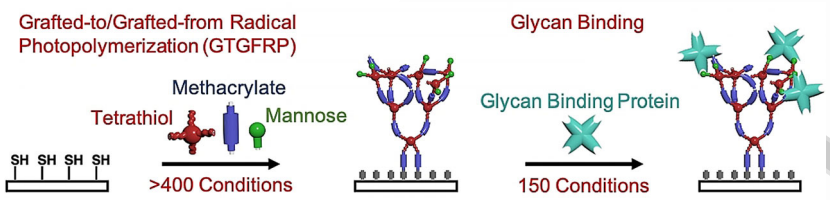

Sub-femtomolar avidity with glycan binding protein is achieved in a glycan microarray architecture that controls precisely carbohydrate density and valency. The biomimetic glycopolymers are prepared via a new surface-initiated polymerization, termed "grafted-to/grafted-from radical photopolymerization" that was optimized using hypersurface photolithography, a printing strategy that substantially accelerates reaction discovery and optimization.

Carbohydrates

D. J. Valles, Y. S. Zholdassov, J. Korpanty, S. Uddin, Y. Naeem, D. R. Mootoo, N. C. Gianneschi, A. B. Braunschweig* ——— ■■■■–■■■■

Glycopolymer Microarrays with Sub-Femtomolar Avidity for Glycan Binding Proteins Prepared by Grafted-To/Grafted-From Photopolymerizations

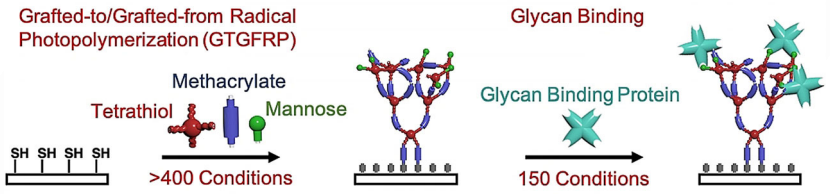

Sub-femtomolar avidity with glycan binding protein is achieved in a glycan microarray architecture that controls precisely carbohydrate density and valency. The biomimetic glycopolymers are prepared via a new surface-initiated polymerization, termed „grafted-to/grafted-from radical photopolymerization" that was optimized using hypersurface photolithography, a printing strategy that substantially accelerates reaction discovery and optimization.

Please check that the ORCID identifiers listed below are correct. We encourage all authors to provide an ORCID identifier for each coauthor. ORCID is a registry that provides researchers with a unique digital identifier. Some funding agencies recommend or even require the inclusion of ORCID IDs in all published articles, and authors should consult their funding agency guidelines for details. Registration is easy and free; for further information, see http://orcid.org/.

Daniel J. Valles http://orcid.org/0000-0001-9510-3042
Yerzhan S. Zholdassov http://orcid.org/0000-0002-0927-3115
Joanna Korpanty http://orcid.org/0000-0002-9274-5936
Samiha Uddin http://orcid.org/0000-0002-0095-0001
Yasir Naeem http://orcid.org/0000-0003-1448-263X
Prof. David R. Mootoo http://orcid.org/0000-0002-5159-1299
Prof. Nathan C. Gianneschi http://orcid.org/0000-0001-9945-5475
Prof. Adam B. Braunschweig http://orcid.org/0000-0003-0344-3029

